Schizophrenia Bulletin vol. 41 no. 1 pp. 123–132, 2015
doi:10.1093/schbul/sbu032
Advance Access publication March 12, 2014

Persistent Infection by HSV-1 Is Associated With Changes in Functional Architecture of iPSC-Derived Neurons and Brain Activation Patterns Underlying Working Memory Performance

Leonardo D'Aiuto[1,10], Konasale M. Prasad[1,10], Catherine H. Upton[1], Luigi Viggiano[2], Jadranka Milosevic[3], Giorgio Raimondi[4], Lora McClain[1], Kodavali Chowdari[1], Jay Tischfield[5], Michael Sheldon[5], Jennifer C. Moore[5], Robert H. Yolken[6], Paul R. Kinchington[7,8], and Vishwajit L. Nimgaonkar[*,1,9]

[1]Department of Psychiatry, WPIC, University of Pittsburgh, School of Medicine, Pittsburgh PA; [2]Department of Biology, University of Bari "Aldo Moro", Bari, Italy; [3]Division of Pulmonary, Allergy and Critical Care Medicine, University of Pittsburgh School of Medicine, Pittsburgh, PA; [4]Department of Plastic and Reconstructive Surgery, Johns Hopkins University School of Medicine, Baltimore, MD; [5]Department of Genetics and The Human Genome Institute of New Jersey, Rutgers, The State University of New Jersey, Piscataway, NJ; [6]Stanley Division of Neurovirology, Department of Pediatrics, Johns Hopkins University School of Medicine, Baltimore, MD; [7]Department of Ophthalmology, University of Pittsburgh School of Medicine, Pittsburgh, PA; [8]Department of Molecular Genetics & Biochemistry, University of Pittsburgh, Pittsburgh, PA; [9]Department of Human Genetics, Graduate School of Public Health, University of Pittsburgh, Pittsburgh, PA

[10]These authors contributed equally to the article.

*To whom correspondence should be addressed; Western Psychiatric Institute and Clinic, TDH 441, 3811 O'Hara St, Pittsburgh, PA 15213, US; tel: 412-246-6353, fax: 412-246-6350, e-mail: vishwajitnl@upmc.edu

Background: **Herpes simplex virus, type 1 (HSV-1) commonly produces lytic mucosal lesions. It invariably initiates latent infection in sensory ganglia enabling persistent, lifelong infection. Acute HSV-1 encephalitis is rare and definitive evidence of latent infection in the brain is lacking. However, exposure untraceable to encephalitis has been repeatedly associated with impaired working memory and executive functions, particularly among schizophrenia patients.** ***Methods*****: Patterns of HSV-1 infection and gene expression changes were examined in human induced pluripotent stem cell (iPSC)-derived neurons. Separately, differences in blood oxygenation level-dependent (BOLD) responses to working memory challenges using letter *n*-back tests were investigated using functional magnetic resonance imaging (fMRI) among schizophrenia cases/controls.** ***Results*****: HSV-1 induced lytic changes in iPSC-derived glutamatergic neurons and neuroprogenitor cells. In neurons, HSV-1 also entered a quiescent state following coincubation with antiviral drugs, with distinctive changes in gene expression related to functions such as glutamatergic signaling. In the fMRI studies, main effects of schizophrenia ($P = .001$) and HSV-1 exposure (1-back, $P = 1.76 \times 10^{-4}$; 2-back, $P = 1.39 \times 10^{-5}$) on BOLD responses were observed. We also noted increased BOLD responses in the frontoparietal, thalamus, and midbrain regions among HSV-1 exposed schizophrenia cases and controls, compared with unexposed persons.** ***Conclusions*****: The lytic/quiescent cycles in iPSC-derived neurons indicate that persistent neuronal infection can occur, altering cellular function. The fMRI studies affirm the associations between nonencephalitic HSV-1 infection and functional brain changes linked with working memory impairment. The fMRI and iPSC studies together provide putative mechanisms for the cognitive impairments linked to HSV-1 exposure.**

Key words: memory/induced pluripotent stem cells/herpes simplex virus type 1/fMRI/herpes

Introduction

Herpes simplex virus, type 1 (HSV-1) causes human specific infections in the majority of US adults (http://www.cdc.gov/nchs/nhanes.htm) and increasing numbers of neonates (http://www.cdc.gov/nchs/nhanes.htm).[1,2] Mucosal lesions such as cold sores occur after primary infection, and recurrent infections can induce blinding stromal keratitis. HSV-1 causes fulminant lytic infection in all human cells except sensory ganglia, where latent infection can be established in neurons that serve as reservoirs for lifelong recurrent infections. Persistent infection is thus marked by sporadic productive, lytic infections alternating with latency, when gene expression is largely

silenced and only the untranslated latency-associated transcripts (LAT) are abundantly expressed.[3]

Periodic reactivation can cause HSV-1 encephalitis, with extensive cognitive impairment, and postencephalitic sequelae.[3] Its rarity (~0.04%) suggests that HSV-1 infection does not ordinarily affect the brain, but viral DNA has been detected in 35% of nonencephalitic postmortem brain tissues,[4,5] suggesting spread to the brain during persistent infection. Mild/moderate impairments in attention, working, and verbal memory untraceable to prior encephalitis or socioeconomic status (SES)[4] were reported repeatedly among HSV-1 exposed schizophrenia patients and even healthy individuals,[6–14] with only one discrepant report.[15] The estimated ORs for cognitive dysfunction among HSV-1–exposed young adults are 1.25–3.2,[12,13] indicating population attributable risks between 15.2%–59.3%. Reduced prefrontal cortical gray matter volume was also reported among HSV-1–exposed schizophrenia patients,[16,17] with progressive cognitive impairments and gray matter loss.[17] The cognitive impairments were alleviated with an antiviral agent in a randomized placebo-controlled trial.[18] These studies together affirm the majority of Bradford-Hill criteria, suggesting causal links.[14]

To generate testable mechanisms for the associations, we investigated cellular models using human induced pluripotent stem cells (iPSCs), because existing HSV-1 models utilize nonhuman tissues or transformed cell lines; such models may not recapitulate human specific infection.[19–21] With functional magnetic resonance imaging (fMRI), we separately evaluated brain activation patterns while participants performed the *n*-back task, a well-established working memory task that identifies consistent patterns of brain activation differences among schizophrenia cases.[22,23]

Methods

iPSC-Based Studies

iPSCs. iPSCs were generated from human skin biopsies. Line 5404 from a schizophrenia patient was used for all experiments. Line HFF1-S, from neonatal foreskin of an anonymous donor was used for confirmatory studies. Neural progenitor cells (NPCs) and glutamatergic neurons[24] were derived from iPSCs[24] (supplementary figures S1 and S2 and supplementary information).

HSV-1 Infection. We used a genetically engineered HSV-1 construct incorporating enhanced green fluorescent protein (EGFP) and monomeric red fluorescent protein (RFP) as reporter genes whose expression is driven by the viral promoters ICP0 and Glycoprotein C, respectively.[25] EGFP expression in infected cells indicates that HSV-1 has entered lytic cycles, while RFP expression indicates commitment to viral DNA replication. Cells were incubated with HSV-1 for 2 h at specified multiplicity of infection (MOI). To inhibit viral replication, cells were preincubated with antivirals used in animal models: acyclovir (50 μM), or (E)-5-(2-bromovinyl)-2′-deoxyuridine (5BVdU, 30 μM) along with interferon-alpha (IFN-α, 125 U/ml).[22] The proportion of cells expressing EGFP and RFP was determined by flow cytometry (FC). Images were acquired using a Leica IL MD LED inverted fluorescence microscope and a Leica DM5500B fluorescence microscope.

Viral Gene Expression. RNA was extracted using Qiagen kits. Complementary DNA was synthesized using total RNA with SuperScript III recommended protocol (Invitrogen) and quantitative PCR (qPCR) performed using the target and reference (beta actin) Taqman probes with Applied Biosystems-recommended protocols (ABI). All experiments were conducted in triplicate and the comparative Ct method used for quantification.[26]

Three-Dimensional Fluorescence In Situ Hybridization. Three-dimensional fluorescence in situ hybridization (3D-FISH) was performed using the HSV-1 genome as a probe.[27] To visualize viral DNA in host cellular nuclei, iPSC-derived neurons were infected after 60 days of differentiation in neurobasal medium on matrigel-coated chamber slides. Neurons were infected with HSV-1 in the presence or absence of 5BVdU+IFN-α at MOI 0.3. On average, 50 nuclei from each cellular preparation were scanned. Digital images were generated using Leica LAS AF, 3D Visualization Module. Hybridization signals were subjected to uniform thresholding to demarcate the signals.

Oligonucleotide Microarray Analyses. Cy3-labeled cRNA was used for hybridization to Agilent Human GE 8x60K V2 Gene Expression microarrays (Agilent Technologies), the microarrays scanned using the Agilent Microarray Scanner and data analyzed with Agilent Feature Extraction software (A 9.1.3).[24] Differentially expressed genes were determined using unpaired *t* tests and Benjamini-Hochberg correction with $P \leq .05$ and the fold change of 2 as thresholds. The data were deposited in NCBI's Gene Expression Omnibus database (http://www.ncbi.nlm.nih.gov/geo/query/acc.cgi?acc=GSE46043).

fMRI Studies

Clinical Evaluations. Participants (schizophrenia = 19, controls = 23) completed the Structured Clinical Interview for DSM-IV[28] followed by consensus diagnoses.[16] SES was evaluated using the Hollingshead Index.[29] Exclusion criteria included substance abuse in the past month or dependence in the last 6 months, history of medical/neurological disorders, mental retardation (DSM-IV), illness duration over 8 years or participation in prior HSV-1 studies. The controls were screened for absence of psychosis and substance abuse.[16] After complete description of the study, written informed consent was obtained.

HSV-1 Exposure. IgG antibodies to HSV-1 were assayed using solid-phase enzyme immunoassays.[14]

MRI Studies. Structural MRI was acquired on a Siemens 3T Tim Trio whole-body scanner using the MPRAGE sequence to co-register fMRI data, overlay the blood oxygenation level-dependent (BOLD) responses and identify regions-of-interest. Scanning parameters were: echo time (TE) = 3.52 ms, repetition time (TR) = 2300 ms, flip angle = 9°, thickness = 0.8 mm, and number of slices = 192.[30] In the same session, subjects performed a letter *n*-back task and whole-brain BOLD responses were collected using gradient-echo echo-planar imaging (EPI). Scanning parameters for the fMRI were: TE = 31 ms, TR = 2000 ms, 36 axial/oblique slices of 4-mm thickness, field of view = 240 mm, flip angle = 80°, and matrix size = 64 × 64. The letter *n*-back task consisted of 6 blocks (2 blocks each of 0-back, 1-back, and 2-back) of English upper case letters as stimuli. Each stimulus was presented for 500 ms. The interstimulus interval (ISI) was jittered randomly between 1.5 and 5.5 s with an average ISI of 3.5 s. Each block was followed by 20 s rest. The first block presented was always 0-back to acclimatize the subjects in the scanner, followed by a randomized order of presentation. Stimuli were presented using E-prime through back projection on a white screen. Subjects responded through a fiber-optic button system by pressing the assigned button every time they saw X on the screen for the 0-back, if they saw the same letter preceding the one presented earlier for the 1-back and if they saw a letter shown 2 letters before the one they were seeing for the 2-back. The responses were collected for both accuracy and response time.

Image Processing. fMRI data were analyzed using SPM8 (http://www.fil.ion.ucl.ac.uk/spm/software/spm8/). Images were realigned and normalized to a standard EPI template and smoothed with 8 × 8 × 8 Gaussian kernel. A full-factorial random effects model was implemented within SPM8 with age, sex, and SES as covariates. We preferred to compare groups across each task level since the behavioral data between-group showed significant differences across each task level rather than between levels of performance. A priori combined intensity and spatial extent threshold significance was determined by running 10 000 Monte Carlo simulations on AlphaSim[31] for the whole brain. The simulation showed that the BOLD differences within a cluster of 1385 contiguous voxels with a minimum voxel-wise difference of $P < .05$, would provide a $P < .05$ corrected for both the intensity and the spatial extent of the clusters. Task performance data were analyzed using generalized linear models for mean response time and the Mann-Whitney *U* tests for accuracy. Percent signal changes were extracted from the regional masks of Brodmann areas (BA) defined by the WFU PickAtlas[32] that contained the peak intensity voxel and were analyzed using ANOVA on SPSS 21.

Results

iPSC-Based Studies

HSV-1 Infection in NPCs and Neurons. At 24 h post-infection (p.i.), FC analysis showed ~30% and ~15% of EGFP-positive ($EGFP^+$) cells in infected NPCs and neurons respectively, indicating lytic infection (figure 1). A ~2-fold reduction of $EGFP^+$ cells was observed in NPCs and ~3-fold reduction in neurons when HSV1-infected cells were coincubated with acyclovir, compared with vehicle-treated controls. Separately, NPCs and neuronal cultures coincubated with 5BVdU and IFN-α showed a greater reduction in $EGFP^+$ cells (~8% and ~2%, respectively), compared with untreated control cells or acyclovir-treated cells, suggesting that the antiviral agents suppressed viral gene expression.

Even in the presence of 5BVdU+IFN-α, the majority of infected NPCs detached from culture plates without a concomitant increase in the frequency of $EGFP^+$ and RFP^+ cells, suggesting that HSV-1 quiescent infection cannot be established consistently in NPCs (figure 2, top panel).

In contrast, when neuronal cultures were infected at MOI of 0.3 with 5BVdU+IFN-α and maintained from day −1 to day +7 p.i., only 9% of cells expressed EGFP, suggesting that viral gene expression was suppressed in the majority of cells and lytic infection was present in a minority (figure 2, middle panel). Infectious viral particles were undetectable in the supernatant for 7 days of infected neuronal cultures treated with inhibitors, based on subsequent Vero cell plaque assays (figure 2, bottom panel, left). Culture supernatants from these neuronal cultures tested against new neuronal cultures (1/20 of the volumes of the culture supernatants were applied to neuronal cultures) failed to yield $EGFP^+$ or $EGFP^+/RFP^+$ cells in all cultures up to 48 h p.i., consistent with the plaque assays (figure 2, bottom panel, right). Though the green fluorescence in the initial neuronal cultures indicates activation of the ICP0 promoter, productive infection was thus fully suppressed and quiescent infection may be present (figure 2, middle panel).

Withdrawal of 5BVdU+IFN-α was followed by ~3-fold increase of $EGFP^+$ cells and ~5-fold increase of $EGFP^+/RFP^+$ cells (figure 2, middle panel). Infectious viral particles were undetected in most cultures, although a relatively low level of infectious virus (~3 log(10) pfu/ml) was detected in 3 out of 9 cultures (data not shown). Culture supernatants were also tested for presence of virions by application to additional neuronal cultures. Only sporadic $EGFP^+$ and $EGFP^+/RFP^+$ cells were observed when neuronal cultures were infected with up to 1/20 of the volume of the culture supernatants (figure 2, bottom panel, right). Thus, withdrawal of 5BVdU and IFN-α reactivates lytic cycle genes, but productive infection is still substantially suppressed.

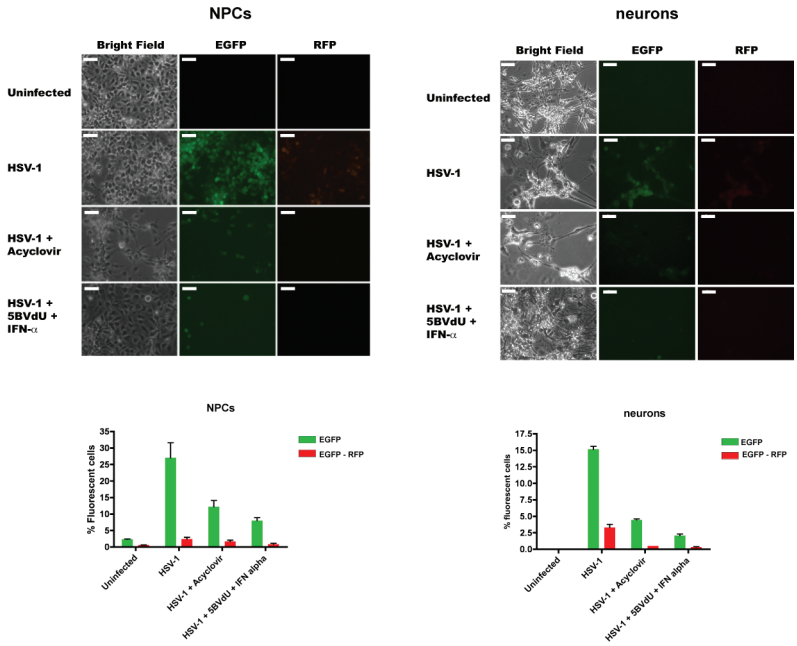

Fig. 1. Comparative efficiency of antiviral drugs to reduce acute infection in induced pluripotent stem-derived neural progenitor cells (NPCs) and neurons. Top panel: microphotographs of NPCs and neuronal cultures infected with herpes simplex virus, type 1 (HSV-1) (multiplicity of infection of 0.1 and 0.3, respectively) in the presence or absence of viral replication inhibitors acyclovir or 5-(E)-5-(2-bromovinyl)-2′-deoxyuridine along with interferon-α. Bottom panel: fluorescence-activated cell sorting analysis of uninfected and HSV-1 infected NPC and neuronal cultures. Scale bar is 50 μm. For a color version, see this figure online.

Reactivation of Quiescent Infection With Sodium Butyrate. Neurons were cultured for 5 days with sodium butyrate (NaB) (5 mM), a histone deacetylase inhibitor, after initial 7-day treatment with 5BVdU+IFN-α. FC showed ~2-fold increase of $EGFP^+$ cells and ~6-fold increase of $EGFP^+/RFP^+$ cells, (figure 2, middle panel). Productive infection was confirmed by applying NaB-treated culture supernatants to fresh neuronal cultures, yielding a high proportion of $EGFP^+$ and EGFP+/RFP^+ cells (figure 2, bottom panel, right). The viral titer of culture supernatant was ~4 log(10) pfu/ml (figure 2, bottom panel, left). Thus, HSV-1 can be recovered from quiescently infected neurons with NaB.

Nuclear Localization of the HSV-1 Genome During Neuronal Infection. Lytic or quiescent infection was induced in iPSC-derived neurons as described and HSV-1 genomes visualized using 3D-FISH. In acutely infected cultures, numerous FISH signals corresponding to HSV-1 genomes were found in the central region of the nucleus, and the host chromatin showed displacement toward the nuclear periphery (supplementary figure S3a). In neurons with quiescent infection, only a weak signal was detected at the nuclear periphery (supplementary figure S3b).

Viral and Neuronal Gene Expression. Using qPCR assays, viral LAT, ICP4, and DNA polymerase genes were expressed at higher levels during lytic vs quiescent infection (fold-changes: LAT: 54, ICP4: 63, DNA polymerase: 51). Microarray analysis of host neuronal gene expression indicated that 10 087 genes were altered significantly during lytic infection ($P < .05$, corrected for multiple comparisons, mean fold changes <0.5 or >2), but during quiescent infection, only 1525 genes changed significantly; the latter included glutamate receptor and voltage-gated ion channel genes (figure 3). During lytic infection, Ingenuity Pathways Analysis indicated enrichment of glutamate receptor signaling, mitochondrial dysfunction, axonal guidance signaling, chondroitin and dermatan sulfate degradation pathways; an overlapping set were altered in quiescently infected cells (figure 3).

fMRI Studies

Participants. HSV-1 exposure was significantly more prevalent among schizophrenia cases ($HSV1^+ = 13$, $HSV1^- = 6$) than healthy controls (HC; $HSV1^+ = 6$, $HSV1^- = 17$; $\chi^2 = 7.53$, $df = 3$, $P = .006$), but the mean age (schizophrenia, 27.44 ± 9.87 years; HC, 26.38 ± 6.78 years, $t = 0.41$, $P = .4$) and gender (schizophrenia, M/F 10/9; HC, M/F 8/15, $\chi^2 = 1.35$, $df = 3$, $P = .25$) distribution did not differ significantly across diagnostic groups or by serological status (all $P > .4$). Although the SES of schizophrenia patients (27.03 ± 8.76) was significantly lower than the HC (41.59 ± 9.01) ($\chi^2 = 5.28$, $P < .001$), it did not differ by HSV-1 status in the case/control groups.

Letter n-*Back Task.* The overall sensitivity of performance (d') was 2.95, with no significant differences across

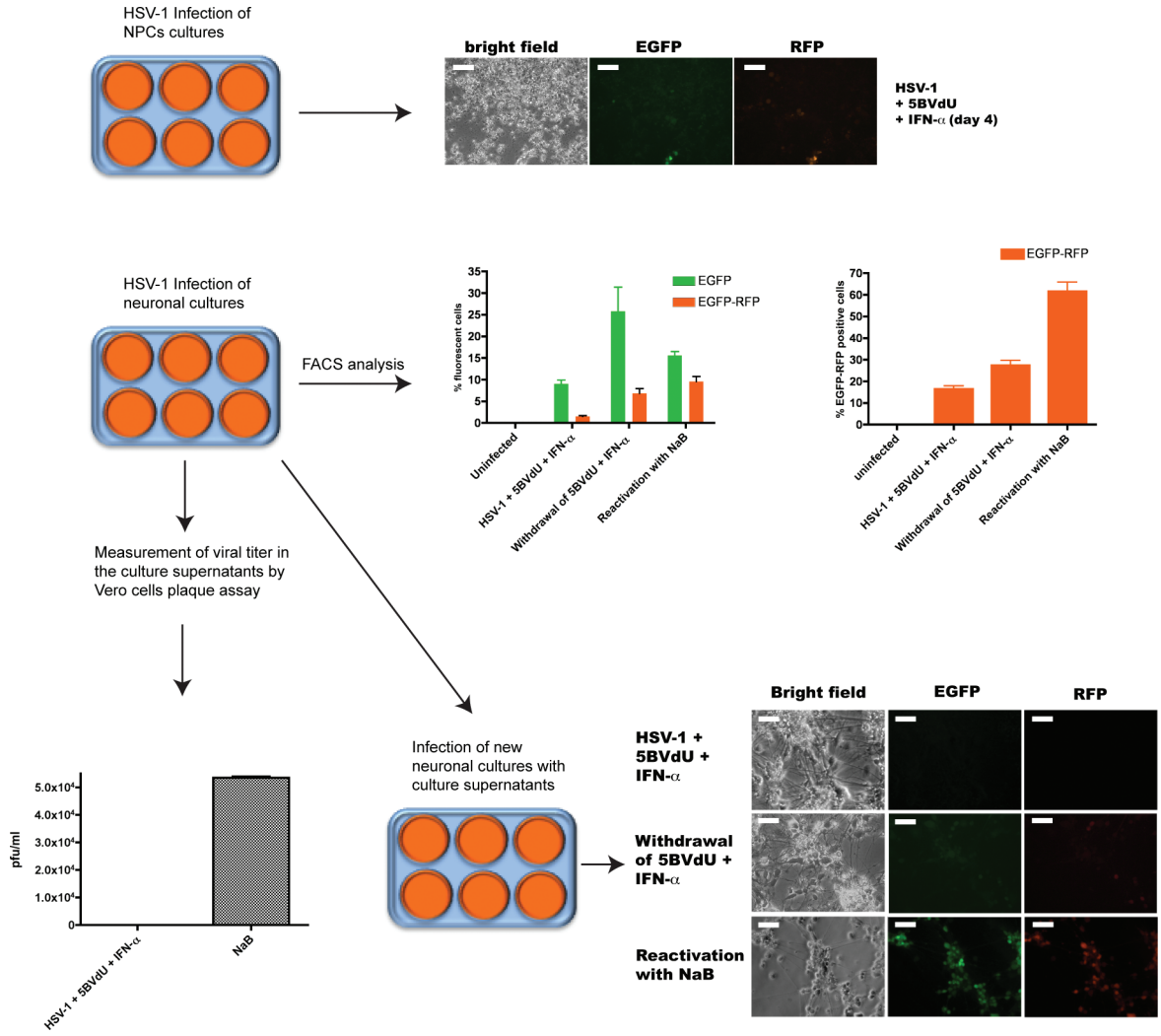

Fig. 2. Quiescent infection established in neurons but not in neural progenitor cells (NPCs). Top panel: microphotographs of induced pluripotent stem-derived NPCs infected with herpes simplex virus, type 1 (HSV-1) in the presence of 5-(E)-5-(2-bromovinyl)-2′-deoxyuridine (5BVdU) and interferon (IFN)-α (5BVdU+IFN-α). Middle and bottom panels: neuronal cultures were incubated under the following conditions: (1) uninfected, (2) infected with HSV-1 and 5BVdU + IFN-α for 7 days ("HSV-1+5BVdU+IFN-α"), (3) infected with HSV-1 and cultured with 5BVdU+IFN-α for 7 days, then drugs were removed from culture medium, and infected cells were further cultured for 5 days in neurobasal medium alone ("withdrawal of 5BVdU+IFN-α"), (4) infected with HSV-1 and cultured with 5BVdU+IFN-α for 7 days, then drugs were removed from culture medium, and infected cells were further cultured for 5 days in neurobasal medium with sodium butyrate (NaB) ("reactivation with NaB"). The relative fraction of enhanced green fluorescent protein$^+$/red fluorescent protein$^+$ cells in each condition is shown (middle panel, right). Viral titer in the supernatants from the culture plates was measured using Vero plaque assays (bottom panel, left). Microphotographs in the bottom panel, right, show the effects of adding supernatants from the original cultures to fresh neuronal cultures (label to left of each microphotograph indicates the culture condition from which the supernatant was derived). Scale bar is 50 µm. For a color version, see this figure online.

diagnostic or serostatus groups. The response time of 0-back (schizophrenia, 676.94 ± 121.25 ms; HC, 627.38 ± 192.77 ms; Wald $\chi^2 = 4.01$, $df = 1$, $P = .045$) and 1-back (schizophrenia, 795.31 ± 181.15 ms; HC, 712.57 ± 275.82 ms; Wald $\chi^2 = 5.94$, $df = 1$, $P = .015$) showed diagnosis effect but not HSV-1 status or diagnosis-by-serostatus interaction effects. The 2-back task response time showed a trend for the main effect of diagnosis (schizophrenia, 895.29 ± 504.43 ms; HC, 825.64 ± 276.44 ms; Wald $\chi^2 = 2.9$, $df = 1$, $P = .088$) and HSV-1 status (HSV1$^+$ = 986.74 ± 527.78 ms; HSV1$^-$ = 712.39 ± 438.30 ms, Wald $\chi^2 = 3.45$, df 1, $P = 0.06$) and diagnosis-by-HSV1 status interaction (Wald $\chi^2 = 3.6$, $df = 1$, $P = .058$). There were no significant main effects of diagnosis, HSV-1 status or diagnosis-by-HSV1 status interaction on accuracy of performance. Besides, we did not observe either diagnosis or HSV1 status effect on mean response times or accuracy between each level of task across the groups. Therefore, the groups were contrasted at each level of task for BOLD response differences.

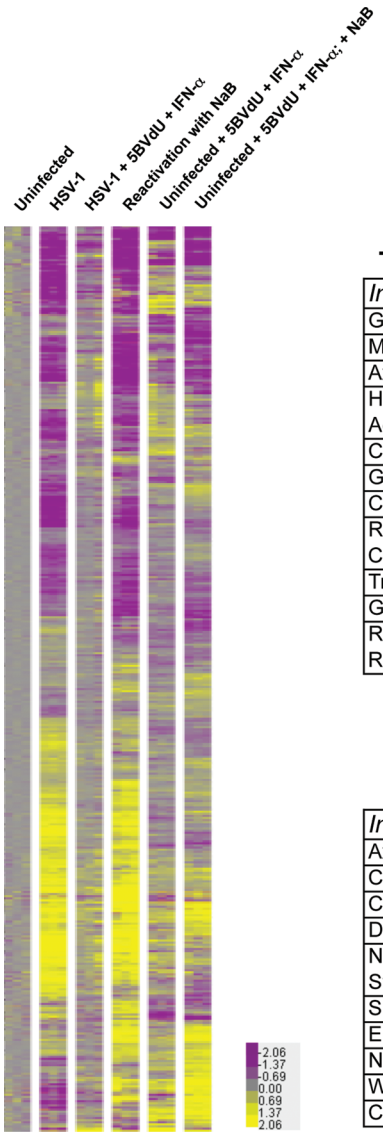

Top Functions affected as a result of HSV-1 lytic infection

Ingenuity Canonical Pathways	*-log(p-value)*	*Ratio*	*P-value*
Glutamate Receptor Signaling	3.64	0.541	2.28E-04
Mitochondrial Dysfunction	3.56	0.49	2.75E-04
Axonal Guidance Signaling	2.81	0.389	1.53E-03
Hepatic Fibrosis / Hepatic Stellate Cell Activation	2.73	0.464	1.88E-03
CREB Signaling in Neurons	2.72	0.422	1.89E-03
Granulocyte Adhesion and Diapedesis	2.31	0.446	4.93E-03
Chondroitin Sulfate Degradation (Metazoa)	2.24	0.75	5.73E-03
Role of Osteoblasts, Osteoclasts and Chondrocytes in Rheumatoid Arthritis	2.21	0.416	6.13E-03
Triacylglycerol Biosynthesis	2.16	0.576	6.85E-03
G Protein Signaling Mediated by Tubby	2.13	0.486	7.48E-03
Role of NFAT in Regulation of the Immune Response	2.08	0.398	8.38E-03

Top Functions affected in quiescent cultures

Ingenuity Canonical Pathways	*-log(p-value)*	*Ratio*	*P-value*
Axonal Guidance Signaling	3.283	0.101	5.21E-04
Chondroitin Sulfate Degradation (Metazoa)	3.182	0.417	6.58E-04
Complement System	3.058	0.242	8.74E-04
Dermatan Sulfate Degradation (Metazoa)	2.995	0.385	1.01E-03
Nitric Oxide Signaling in the Cardiovascular System	2.88	0.147	1.32E-03
Superpathway of Cholesterol Biosynthesis	2.837	0.259	1.46E-03
Ephrin Receptor Signaling	2.341	0.107	4.56E-03
NF-κB Signaling	2.309	0.118	4.90E-03
Wnt/β-catenin Signaling	2.163	0.118	6.87E-03
Caveolar-mediated Endocytosis Signaling	2.145	0.136	7.15E-03

Fig. 3. Gene expression analysis in acutely and quiescently infected neurons. The heat map represents statistically significant ($P \leq .05$), differentially expressed genes after one-way ANOVA analysis and Benjamini-Hochberg correction applied. Columns represent individual samples (each group $n = 3$); selected genes are represented in rows. Upregulated genes are shown in yellow, and downregulated genes are shown in purple. Right: Ingenuity Pathways Analysis of acutely and quiescently infected neuronal cultures. For a color version, see this figure online.

BOLD Response Differences (figure 4)

Main Effect of Task, Diagnostic Status, and HSV-1 Status. Task Main Effect The task main effect was noted in the prefrontal (BA 10, 45 and anterior cingulate gyrus,), posterior parietal cortex (BA 40), occipital and insular cortices for the 1-back, and the prefrontal (BA 8 and 10), posterior parietal (BA 40), occipital and inferior temporal cortices for the 2-back, but not for the 0-back task where only the occipital cortex (BA 17 and 18) showed increased activations.

HSV-1 Main Effect A significant effect of HSV-1 exposure was noted in the prefrontal and subcortical regions for the 1-back (BA 8) and 2-back (BA 6, 8, left thalamus, substantia nigra, and red nucleus), but not for the 0-back.

Diagnosis Main Effect 0-back did not show diagnosis main effect. We observed diagnosis main effect for 1-back in the inferior parietal lobule (BA 40), and for the 2-back task in the superior temporal gyrus (STG, BA 42, 22), and the right cuneus, but not in the prefrontal regions at the combined intensity and spatial extent threshold used here.

Diagnosis-by-HSV-1 Interactions A significant interaction was noted in the left superior parietal lobule (BA 7, $F = 16.30$, $P = 3.02 \times 10^{-4}$) for the 0-back, but not for the 1-back and 2-back tasks.

Associations With HSV-1 Status. The *t* tests to investigate directionality of effects showed increased BOLD

Table 1. fMRI Results With Contrasts

Contrast	*x*	*y*	*z*	Region	Brodmann Area	Statistic	Corrected *P*
Main effect of task							
1 back	−30	22	4	Left inferior frontal gyrus, insula	45, 47, 13	40.16	3.59×10^{-7}
	2	56	2	Bilateral medial frontal, superior frontal, and anterior cingulate	10	37.12	7.34×10^{-7}
	40	−46	44	Right inferior parietal lobule and subgyral	40	19.85	9.10×10^{-5}
2-back	56	−4	−30	Right fusiform, inferior temporal, and middle temporal gyri	20, 21	33.53	1.79×10^{-6}
	−36	−52	56	Left inferior parietal lobule	40	42.51	2.10×10^{-7}
	48	14	38	Right middle frontal gyrus	8, 10, 46	83.06	1.57×10^{-10}
	−2	56	4	Left medial frontal gyrus	10, 11, 32	44.19	1.45×10^{-7}
Main effect of HSV1 serostatus							
1-back	−4	26	64	Left superior frontal gyrus	6	17.87	1.76×10^{-4}
2-back	−12	−22	−10	Left thalamus	—	26.45	1.39×10^{-5}
	−22	−2	68	Left superior and middle frontal gyrus	6	25.97	1.21×10^{-5}
Main effect of diagnosis							
1-back	−62	−36	34	Left inferior parietal lobule	40	13.92	.001
2-back	−62	−18	8	Left transverse temporal and superior temporal gyrus	22, 41, 42	25.02	1.83×10^{-5}
Pooled sample of SZ and HC ($HSV1^+ > HSV1^-$)							
1-back	−4	26	64	Left superior and medial frontal gyrus, anterior cingulate	6, 8, 32	**4.23**	8.79×10^{-5}
	−2	−26	8	Left thalamus	—	2.89	.003
2-back	−12	22	−10	Left thalamus, substantia nigra, and bilateral red nucleus	—	5.10	6.94×10^{-6}
	−22	−2	68	Left frontal lobe, superior frontal gyrus	6	5.14	6.06×10^{-6}
Within SZ subjects ($HSV1^+ > HSV1^-$)							
1-back	20	22	66	Right middle frontal gyrus and right superior frontal gyrus	6	4.61	2.90×10^{-5}
2-back	−2	−20	−12	Bilateral red nucleus, brainstem, and midbrain	—	4.17	1.02×10^{-4}
Within HC subjects ($HSV1^+ > HSV1^-$)							
1-back	−2	4	38	Bilateral cingulate gyrus	24, 32	3.24	.001
2-back	62	−58	12	Right superior temporal gyrus, right middle temporal gyrus	21,22,39	4.51	3.86×10^{-5}
	−20	−4	70	Left superior frontal gyrus	6, 9, 32	3.73	3.32×10^{-4}
	6	−10	4	Left medial dorsal, ventral lateral, and anterior nuclei of thalamus	—	3.73	3.64×10^{-4}
Between $HSV1^+$ SZ and $HSV1^+$ HC ($HSV1^+$ SZ > HC)							
1-back	4	−76	4	Right cuneus and lingual	17, 18, 23, 30	3.76	3.31×10^{-4}
2-back	26	−70	−10	Right fusiform gyrus and lingual gyrus	18, 19	4.24	8.55×10^{-5}
Between $HSV1^+$ SZ and $HSV1^+$ HC ($HSV1^+$ SZ < HC)							
2-back	−24	6	56	Left superior and middle frontal gyrus	6, 24, 32	3.26	.001
Between $HSV1^-$ SZ and $HSV1^-$ HC ($HSV1^-$ SZ > HC)							
1-back	4	−4	30	Bilateral limbic lobe, bilateral cingulate gyrus	24	4.07	1.36×10^{-4}
2-back	−60	−26	4	Left superior temporal gyrus, left middle temporal gyrus	21, 22, 41, 42	3.63	4.71×10^{-4}
	34	54	30	Right superior frontal gyrus, right middle frontal gyrus[a]	9, 10	3.69	3.97×10^{-4}
	8	−12	60	Right medial frontal gyrus	6	3.53	.001
	60	−58	10	Right superior temporal gyrus, right middle temporal gyrus	21, 22, 39	3.39	.001

Note: BA, Brodmann area; fMRI, functional magnetic resonance imaging; HC, healthy control; HSV1, herpes simplex virus, type 1; SZ, schizophrenia.
[a]BA 9 and 10 was significant when the cluster size was reduced to 1343 voxels that corresponded to corrected $P < .06$. All other regions were examined at cluster size of 1385 that corresponded to corrected $P < .05$.

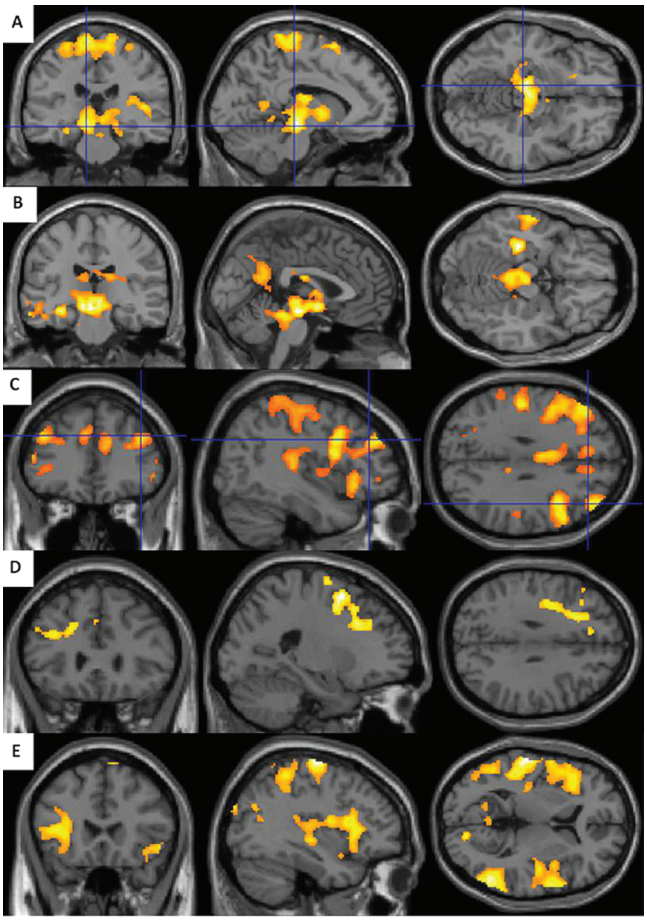

Fig. 4. Blood oxygenation level dependent (BOLD) response differences in response to 2-back challenge. (A) Combined schizophrenia and healthy control sample. Herpes simplex virus, type 1 (HSV1)$^+$ show greater activation compared with HSV-1$^-$ subjects in the substantia nigra, the red nucleus, and thalamus. (B) HSV1$^+$ schizophrenia subjects show increased activation in bilateral red nucleus and substantia nigra compared with HSV1$^-$ schizophrenia subjects. (C) Increased activation in the prefrontal and parietal regions among HSV1$^+$ in controls compared with HSV1$^-$ controls. (D) HSV1$^+$ schizophrenia subjects showed decreased BOLD responses in the anterior cingulate regions compared with HSV1$^+$ HC. (E) HSV1$^-$ schizophrenia subjects showing increased BOLD responses in bilateral superior temporal gyri. Increased activation in the prefrontal Brodmann areas 9 and 46 showed a trend (corrected $P = .06$). For a color version, see this figure online.

responses for all contrasts comparing HSV-1–exposed subjects with those not exposed.

Combined Schizophrenia and HC Controlling for Diagnostic Status HSV-1 exposure was associated with increased BOLD responses in the prefrontal and subcortical regions for the 1-back (BA 6, 8, 32, thalamus) and 2-back (BA 6, thalamus, substantia nigra, and red nucleus) tasks, but not for the 0-back task where BOLD responses were increased mainly in the bilateral superior temporal gyri (BA 42, 22, and 40) (table 1). BOLD responses for 1-back task was elevated nearly 2.5-fold in the thalamus ($t = 2.5$, $P = .016$) among HSV1$^+$ compared with HSV1$^-$ subjects. For the 2-back task, HSV1$^+$ subjects showed 3-fold increase in BOLD responses compared with HSV1$^-$ within the substantia nigra, thalamus, and red nucleus cluster ($t = 3.9$, $P = .0003$) (table 1).

BOLD Responses Within and Across Schizophrenia/HC Groups, Grouped by Serological Status. Within schizophrenia subjects, HSV-1 exposure was associated with increased BOLD responses in the BA 6, and the red nucleus, the substantia nigra, the left parahippocampal regions for 1-back and 2-back tasks, respectively (supplementary table 1). In contrast, HSV-1–exposed HC showed increased BOLD responses in the anterior cingulate gyrus (BA 24 and 32), prefrontal (BA 6, 9), and temporal cortices compared with HSV1$^-$ HC. The BOLD responses were decreased in the anterior cingulate region (BA 24 and 32) and BA 6 among HSV1$^+$ schizophrenia subjects compared with HSV1$^+$ HCs for the 2-back task. schizophrenia-HC comparisons among HSV-1–negative individuals showed increased BOLD responses in schizophrenia subjects in the anterior cingulate (BA 24) for the 1-back and in BA 9, 10 and bilateral superior temporal gyri for the 2-back tasks.

Discussion

The iPSC-derived neurons recapitulate lytic HSV-1 infection and can be induced into a quiescent, persistent, reactivable infection. Like established animal models, quiescent infection is accompanied by reduced viral replication, retention of the viral genome in the nucleus, lack of infectious virions, expression of LATs[19–21,33–38] in neurons. Quiescent infection was not observed in NPCs. During lytic infection, microarray analyses showed extensive changes in cognition-related pathways, such as glutamate and cAMP response element-binding protein (CREB) signaling. Fewer changes occurred in quiescent infection, but they too included cognition-relevant glutamate receptor and ion channel genes. We therefore propose a model in which persistent infection occurs in brain neurons similar to that in sensory ganglia, and over time impairs neuronal function (suggested by altered gene expression) without producing florid encephalitis; the altered function may underlie observed cognitive deficits. The relatively high sensitivity of NPCs to HSV-1 infection also suggests that individuals infected in childhood can experience cognitive impairment secondary to altered NPC proliferation and differentiation[39] suggesting the neurodevelopmental implications of HSV-1 exposure. This model needs to be tested and immunological/glial responses explored; simultaneous in vitro and MRI studies in the same persons may also be worthwhile.

The fMRI results suggest increased processing time for working memory performance associated with schizophrenia and HSV-1 exposure. The 2-back mean

response time showed a trend toward significance for the diagnosis, HSV-1 status, and diagnosis-by-HSV-1 exposure interaction, with nonsignificant differences in accuracy of performance. fMRI data mainly showed increased BOLD responses among both schizophrenia and HSV-1–exposed individuals suggesting that an increased neurobiological effort in the prefrontal cortex (PFC), posterior parietal cortex, hippocampus/parahippocampus, thalamus, substantia nigra, and superior temporal lobes is needed to achieve accuracy of working memory performance comparable to unexposed participants. Notably, the HSV-1-exposed individuals showed BOLD responses in the midbrain regions and thalamus. The trigeminal nucleus that receives neuronal inputs from the trigeminal ganglion is situated close to the red nucleus and substantia nigra, and projects to the thalamus. Increased BOLD response in these regions raises the possibility of altered dopamine transmission among HSV-1–exposed subjects. The increased activation in the STG is notable since this region is markedly affected during HSV-1 encephalitis.[3] HSV-1–exposed HC showed activation differences in the classical working memory network that include prefrontal cortex and posterior parietal cortex, whereas HSV-1–exposed schizophrenia subjects recruited regions outside this network (substantia nigra where dopamine neurons are situated, red nucleus, thalamus, and superior temporal gyrus) to perform at the same level as HC. Besides, HSV-1-exposed schizophrenia subjects showed similar prefrontal activations compared to HSV-1 unexposed schizophrenia subjects while performing on par with them, possibly by recruiting other networks involving STG and subcortical structures.

Some shortcomings should be noted. Though functional,[24] the iPS-derived neurons cannot completely recapitulate the milieu interior of the human brain. The fMRI studies did not show diagnosis effects at the PFC; possibly reflecting inadequate power since lowering the statistical threshold to $P < .06$ corrected for intensity and spatial extent shows diagnosis effect. Because HSV-1 virions are usually undetectable in serum,[3] HSV-1 exposure was indexed through serum antibody assays in the fMRI studies.

In conclusion, HSV-1 induces quiescent infection in human iPSC-derived neurons that resembles animal models of latent infection. The fMRI studies indicate increased hemodynamic responses during working memory challenge among HSV-1–exposed individuals without prior encephalitis. We propose specific testable cellular and other models for the published HSV-1–associated cognitive dysfunction.

Supplementary Material

Supplementary material is available at http://schizophreniabulletin.oxfordjournals.org.

Funding

MH 63480 (V.L.N.); MH72995 MH 93540 and the American Psychiatric Institute for Research and Education-Lilly Award (K.M.P.); EY08098 (P.R.K.); and Stanley Medical Research Institute (07R-1712 to V.L.N.).

Acknowledgments

We thank our study participants and research staff. Dr R.H.Y. is a member of the Stanley Medical Research Institute (SMRI) Board of Directors and Scientific Advisory Board. The terms of this arrangement are being managed by the Johns Hopkins University. The authors have declared that there are no conflicts of interest in relation to the subject of this study.

References

1. Gupta R, Warren T, Wald A. Genital herpes. *Lancet*. 2007;370:2127–2137.
2. Flagg EW, Weinstock H. Incidence of neonatal herpes simplex virus infections in the United States, 2006. *Pediatrics*. 2011;127:e1–e8.
3. Steiner I, Kennedy PG, Pachner AR. The neurotropic herpes viruses: herpes simplex and varicella-zoster. *Lancet Neurol*. 2007;6:1015–1028.
4. Baringer JR, Pisani P. Herpes simplex virus genomes in human nervous system tissue analyzed by polymerase chain reaction. *Ann Neurol*. 1994;36:823–829.
5. Karatas H, Gurer G, Pinar A, et al. Investigation of HSV-1, HSV-2, CMV, HHV-6 and HHV-8 DNA by real-time PCR in surgical resection materials of epilepsy patients with mesial temporal lobe sclerosis. *J Neurol Sci*. 2008;264:151–156.
6. Dickerson FB, Boronow JJ, Stallings C, Origoni AE, Ruslanova I, Yolken RH. Association of serum antibodies to herpes simplex virus 1 with cognitive deficits in individuals with schizophrenia. *Arch Gen Psychiatry*. 2003;60:466–472.
7. Shirts BH, Prasad KM, Pogue-Geile MF, Dickerson F, Yolken RH, Nimgaonkar VL. Antibodies to cytomegalovirus and herpes simplex virus 1 associated with cognitive function in schizophrenia. *Schizophr Res*. 2008;106:268–274.
8. Yolken RH, Torrey EF, Lieberman JA, Yang S, Dickerson FB. Serological evidence of exposure to herpes simplex virus type 1 is associated with cognitive deficits in the CATIE schizophrenia sample. *Schizophr Res*. 2011;128:61–65.
9. Schretlen DJ, Vannorsdall TD, Winicki JM, et al. Neuroanatomic and cognitive abnormalities related to herpes simplex virus type 1 in schizophrenia. *Schizophr Res*. 2010;118:224–231.
10. Dickerson F, Stallings C, Origoni A, Vaughan C, Khushalani S, Yolken R. Additive effects of elevated C-reactive protein and exposure to herpes simplex virus type 1 on cognitive impairment in individuals with schizophrenia. *Schizophr Res*. 2012;134:83–88.
11. Dickerson FB, Boronow JJ, Stallings C, et al. Infection with herpes simplex virus type 1 is associated with cognitive deficits in bipolar disorder. *Biol Psychiatry*. 2004;55:588–593.
12. Watson AM, Prasad KM, Klei L, et al. Persistent infection with neurotropic herpes viruses and cognitive impairment. *Psychol Med*. 2013;43:1023–1031.

13. Dickerson F, Stallings C, Sullens A, et al. Association between cognitive functioning, exposure to herpes simplex virus type 1, and the COMT Val158Met genetic polymorphism in adults without a psychiatric disorder. *Brain Behav Immun*. 2008;22:1103–1107.
14. Prasad KM, Watson AM, Dickerson FB, Yolken RH, Nimgaonkar VL. Exposure to herpes simplex virus type 1 and cognitive impairments in individuals with schizophrenia. *Schizophr Bull*. 2012;38:1137–1148.
15. Aiello AE, Haan MN, Pierce CM, Simanek AM, Liang J. Persistent infection, inflammation, and functional impairment in older Latinos. *J Gerontol A Biol Sci Med Sci*. 2008;63:610–618.
16. Prasad KM, Shirts BH, Yolken RH, Keshavan MS, Nimgaonkar VL. Brain morphological changes associated with exposure to HSV1 in first-episode schizophrenia. *Mol Psychiatry.* 2007;12:105–13, 1.
17. Prasad KM, Eack SM, Goradia D, et al. Progressive gray matter loss and changes in cognitive functioning associated with exposure to herpes simplex virus 1 in schizophrenia: a longitudinal study. *Am J Psychiatry*. 2011;168:822–830.
18. Prasad KM, Eack SM, Keshavan MS, Yolken RH, Iyengar S, Nimgaonkar VL. Antiherpes virus-specific treatment and cognition in schizophrenia: a Test-of-Concept Randomized Double-Blind Placebo-Controlled Trial. *Schizophr Bull*. 2012;39:857–866.
19. Bloom DC, Giordani NV, Kwiatkowski DL. Epigenetic regulation of latent HSV-1 gene expression. *Biochim Biophys Acta*. 2010;1799:246–256.
20. Nicoll MP, Proença JT, Efstathiou S. The molecular basis of herpes simplex virus latency. *FEMS Microbiol Rev*. 2012;36:684–705.
21. Giordani NV, Neumann DM, Kwiatkowski DL, et al. During herpes simplex virus type 1 infection of rabbits, the ability to express the latency-associated transcript increases latent-phase transcription of lytic genes. *J Virol.* 2008;82:6056–6060.
22. Carter CS, Perlstein W, Ganguli R, Brar J, Mintun M, Cohen JD. Functional hypofrontality and working memory dysfunction in schizophrenia. *Am J Psychiatry*. 1998;155:1285–1287.
23. Friedman HR, Goldman-Rakic PS. Coactivation of prefrontal cortex and inferior parietal cortex in working memory tasks revealed by 2DG functional mapping in the rhesus monkey. *J Neurosci.* 1994;14:2775–2788.
24. D'Aiuto L, Di Maio R, Heath B, et al. Human induced pluripotent stem cell-derived models to investigate human cytomegalovirus infection in neural cells. *PLoS One*. 2012;7:e49700.
25. Ramachandran S, Knickelbein JE, Ferko C, Hendricks RL, Kinchington PR. Development and pathogenic evaluation of recombinant herpes simplex virus type 1 expressing two fluorescent reporter genes from different lytic promoters. *Virology*. 2008;378:254–264.
26. Talkowski ME, McCann KL, Chen M, et al. Fine-mapping reveals novel alternative splicing of the dopamine transporter. *Am J Med Genet B Neuropsychiatr Genet*. 2010;153B:1434–1447.
27. Cremer M, Müller S, Köhler D, Brero A, Solovei I. Cell preparation and multicolor FISH in 3D preserved cultured mammalian cells. *CSH Protoc.* 2007;2007:pdb.prot4723.
28. First MB, Spitzer RL, Gibbon M, Williams JBW. *Structured Clinical Interview for DSM-IV Axis I Disorders -- Clinical Version (SCID -- I/CV)*. Washington, DC: American Psychiatric Press; 1997.
29. Hollingshead AB. *Four-Factor Index of Social Status*. New Haven, CT: Yale University; 1975.
30. Stolz E, Pancholi KM, Goradia DD, et al. Brain activation patterns during visual episodic memory processing among first-degree relatives of schizophrenia subjects. *Neuroimage*. 2012;63:1154–1161.
31. Maldjian JA, Laurienti PJ, Kraft RA, Burdette JH. An automated method for neuroanatomic and cytoarchitectonic atlas-based interrogation of fMRI data sets. *Neuroimage*. 2003;19:1233–1239.
32. Ward BD. *Simultaneous Inference for fMRI Data*. Milwaukee, WI: University of Wisconsin; 2000.
33. Margolis TP, Elfman FL, Leib D, et al. Spontaneous reactivation of herpes simplex virus type 1 in latently infected murine sensory ganglia. *J Virol.* 2007;81:11069–11074.
34. Liu T, Khanna KM, Chen X, Fink DJ, Hendricks RL. CD8(+) T cells can block herpes simplex virus type 1 (HSV-1) reactivation from latency in sensory neurons. *J Exp Med*. 2000;191:1459–1466.
35. Matthews JT, Terry BJ, Field AK. The structure and function of the HSV DNA replication proteins: defining novel antiviral targets. *Antiviral Res*. 1993;20:89–114.
36. De Clercq E. (E)-5-(2-bromovinyl)-2'-deoxyuridine (BVDU). *Med Res Rev*. 2005;25:1–20.
37. Kramer MF, Cook WJ, Roth FP, et al. Latent herpes simplex virus infection of sensory neurons alters neuronal gene expression. *J Virol.* 2003;77:9533–9541.
38. Kosz-Vnenchak M, Coen DM, Knipe DM. Restricted expression of herpes simplex virus lytic genes during establishment of latent infection by thymidine kinase-negative mutant viruses. *J Virol.* 1990;64:5396–5402.
39. Regnell CE, Hildrestrand GA, Sejersted Y, et al. Hippocampal adult neurogenesis is maintained by Neil3-dependent repair of oxidative DNA lesions in neural progenitor cells. *Cell Rep*. 2012;2:503–510.